Reynolds number effect on the wake of two staggered cylinders

Y. Zhou,[1,a] S. X. Feng,[2] Md. Mahbub Alam,[1] and H. L. Bai[1]
[1]*Department of Mechanical Engineering, The Hong Kong Polytechnic University, Kowloon, Hong Kong*
[2]*Department of Water Environment, Institute of Water Resources and Hydropower Research, Beijing, People's Republic of China*

(Received 20 August 2009; accepted 23 October 2009; published online 29 December 2009)

This work aims to investigate, based on the measured/reported Strouhal number (St) and the flow structure, the Reynolds number (Re) effect on the wake of two identical cylinders with a diameter of d over $P^*=P/d=1.2–4.0$ and $\alpha=0°–90°$, where P is the center-to-center spacing between the two cylinders and α is the angle of incident flow with respect to the line through the two cylinder centers. The Re range examined is from 1.5×10^3 to 2.0×10^4. Two hotwires were used to measure St simultaneously behind each of the two cylinders. The St-Re relationship is classified into four distinct types, i.e., types 1–4. Each is linked to distinct initial conditions, viz., interactions between the four shear layers around the cylinders. Type 1 occurs at small P^*, not exceeding 1.25. The two cylinders act like a single body, producing a single St across the wake throughout the range of Re examined. On the other hand, type 2 occurs at small α ($<10°$). Although single valued, the St in type 2 displays a sudden jump with increasing Re due to a switch in the shear layer, separated from the upstream cylinder, from overshooting to reattachment on the downstream cylinder (type 2A) or from reattachment to coshedding vortices (type 2B), depending on P^*. Type 3 is in the region of intermediate P^* [(1.2–1.5)–2.2] and α (10°–75°). Two distinct St occur at low Re. The lower and the higher ranges of St are associated with the downstream and upstream cylinders, respectively. With increasing Re, the higher St collapses to the lower, which is attributed to a change in the inner shear layer, separated from the upstream cylinder, from squeezing through the gap between cylinders to reattachment on the downstream cylinder. Type 4 occurs at large P^* ($>1.2–2.2$) and again exhibits at low Re two St, above and below the Strouhal number St_0 in the wake of an isolated cylinder, both changing suddenly or progressively to St_0 with increasing Re, which results from a change in the inner shear layer, separated from the upstream cylinder, from reattachment on the downstream cylinder to forming vortices between the cylinders. These types of Re-St relationships are also connected to the flow structure modes reported in literature. The dependence of the St and St-Re relationships on P^* and α is provided, which may be used for the prediction of St in related problems. © *2009 American Institute of Physics*. [doi:10.1063/1.3275846]

I. INTRODUCTION

Multiple slender structures are widely seen in engineering, e.g., chimney stacks, tube bundles in heat exchangers, chemical reaction towers, offshore structures, and skyscrapers in modern cities. Two fluid-dynamically interfering cylinders may be considered as the basic element of multiple structures and the knowledge of this flow is insightful for understanding that around more structures. As such, the flow around two cylinders has received a great deal of attention in literature.

The flow behind two cylinders has been previously classified based on P^* and α, where P is the center-to-center cylinder spacing, α is the angle between the free-stream flow and the line connecting the cylinder centers, and the asterisk stands for normalization by the cylinder diameter d and/or free-stream velocity U_∞. Zdravkovich[1] examined the data reported in literature and divided the possible arrangements of two cylinders into four regions: (i) the proximity interference region, where two cylinders are close to each other and neither is submerged in the wake of the other; (ii) the wake interference region, where the near wake of the upstream cylinder is unaffected by the downstream one but the latter is greatly influenced by the former; (iii) the proximity and wake interference region, where both proximity and wake interference are significant; (iv) no interference region, where the wake of one cylinder does not affect the other. Sumner *et al.*[2] conducted flow visualization and particle image velocimetry (PIV) measurements for $P^*=1.0–5.0$, $\alpha=0°–90°$, and $\mathrm{Re}=850–1900$ ($\mathrm{Re}=U_\infty d/\nu$, where ν is the kinematic viscosity), and divided the P^*-α plane into three: (1) the single-body flow regime, $P^*=1.0–1.125$ and $\alpha=0°–90°$, where two cylinders act like an isolated body with a single vortex-shedding frequency; (2) the small incidence angle regime, $P^*>1.125$ and $\alpha=0°–20°$, where shear layer reattachment or the impingement of vortices onto the downstream cylinder takes place; (3) the large incidence angle regime, $P^*>1.125$, $\alpha=20°–90°$, where vortex pairing, splitting, enveloping, and synchronizing occur. Gu and Sun[3] measured the time-averaged pressure on two cylinders ($P^*=1.1–3.5$ and $\alpha=0°–90°$) at $\mathrm{Re}=(2.2–3.3)\times10^5$, and observed three distinct pressure distributions: patterns I_B, II_B, and III_B on the downstream cylinder, which occurred over $\alpha=0°–9.65°$, 9.7°–15°, and 16°–90°, respectively, at P^*

[a]Author to whom correspondence should be addressed. Electronic mail: mmyzhou@polyu.edu.hk.

 © 2009 American Institute of Physics

Downloaded 17 Mar 2011 to 158.132.161.180. Redistribution subject to AIP license or copyright; see http://pof.aip.org/about/rights_and_permissions

=0.7. The downstream cylinder was completely and partially submerged in the wake of the other, respectively, in patterns I_B and II_B but not in pattern III_B.

Kiya *et al.*[4] measured St behind two cylinders over $P^*=1.0-5.5$ and $\alpha=0°-180°$ with an increment of $\Delta\alpha=15°$ ($Re=1.58\times10^4$). The isocontours of St were given and five regions were identified based on the measured St with reference to that, St_0, in an isolated cylinder wake. Their $\Delta\alpha$ seems too large since the flow is highly sensitive to α and P^* for $\alpha<20°$ and $P^*<2$,[2,3,5,6] which implies the possible loss of important details on St. In their investigation of two staggered cylinders at $Re=(3.2-7.4)\times10^4$, Sumner and Richards[7] observed two distinct St values in both upstream- and downstream-cylinder-generated wakes for some P^* and α ranges (e.g., $P^*=1$, $\alpha=16°-75°$), although the flow physics behind was not discussed. Alam and Sakamoto[8] ascribed this observation to the occurrence of a tristable flow state, i.e., the flow with higher and lower St in the upstream- and downstream-cylinder-generated wakes, respectively, the flow with the higher St in both wakes, and the flow with the lower St in both wakes. The two inner shear layers between the cylinders interact and lead to an intermittent lock-in of the two wakes, thus generating the second and the third flow states. At $x^*\geq2.5$ (where x is the downstream distance from the mid point between the cylinders), Hu and Zhou[6,9] studied experimentally the flow structure and St and their downstream evolution for $P^*=1.2-4.0$ and $\alpha=0°-90°$ ($Re=7.0\times10^3$). Their increments ΔP^* and $\Delta\alpha$ were 0.5 and 10°, respectively. They observed two single-street modes, i.e., S-I and S-II. The two rows of vortices had almost the same strength for S-I but not for S-II. Two twin-street modes, i.e., T-I and T-II, were also observed. The T-I mode was characterized by two streets of different vortex strengths and the T-II mode by two streets of almost the same vortex strength.

The above investigations have been performed at a given Re or a very limited range of Re. On the other hand, a number of previous studies, although done mostly for either the in-tandem ($\alpha=0°$) or side-by-side ($\alpha=90°$) arrangement, did unveil that the Re effect could not be overlooked. Igarashi[10,11] examined the Re effects in the wake of two tandem cylinders on St and pressure fluctuations for $Re=(8.7\times10^3)-(5.2\times10^4)$, and noted that with increasing Re, the pressure fluctuation on the cylinder surfaces increased and St decreased greatly from $Re=1\times10^4$ to 4×10^4. Ljungkrona and Sundén's[12] flow visualization and pressure distribution measurements in the wake of two tandem cylinders [$P^*=1.25-4.0$ and $Re=(3.0\times10^3)-(4.0\times10^4)$] indicated a dependence on Re of the critical P^*, at which a bistable flow occurred and the shear layers separating from the upstream cylinder changed from reattachment upon the downstream cylinder to the rollup, forming vortices, in the gap of the cylinders. Xu and Zhou[13] studied systematically the dependence of St on Re as well as on P^* in the wake of two tandem cylinders [$P^*=1-15$ and $Re=(8.0\times10^2)-(4.2\times10^4)$] and found a new bistable phenomenon, at which the shear layer separated from the upstream cylinder switched from rollup behind to the reattachment onto the downstream cylinder. The occurrence of both bistable phenomena varied appreciably with Re. Kim and Durbin[14] studied the wake of two side-by-side cylinders in the so-called flopping regime ($P^*=1.75$) and observed a variation in the base pressure and St as Re varied from 2.0×10^3 to 7.0×10^3. They further found that the nondimensional mean interval between flips decreased nearly exponentially with increasing Re. Xu *et al.*[15] examined the Re effect, over $Re=(1.5\times10^2)-(1.43\times10^4)$, on the wake of two side-by-side cylinders with $P^*=1.2-1.6$. It was found that an increase in Re could result in a qualitative change in the flow structure; for instance, the wake might alter from a single vortex street behind the cylinders to two streets, one narrow and one wide.

The information available on the Re effect in the wake of two staggered cylinders is very limited. This work aims to fill, at least partially, this gap in literature and to investigate the effect of Re on the flow structure of two staggered cylinders over $Re=(1.5\times10^3)-(2.0\times10^4)$ based on St, as measured using two hotwires. The configurations of the cylinders covered $P^*=1.2-4.0$ and $\alpha=0°-90°$. Experimental details are given in Sec. II. A validation of the present measurement is provided in Sec. III based on the data of the inline and side-by-side arrangements in literature. The dependence of St, flow structure, and the St-Re relationship, along with its classification, on P^* and α is presented and discussed in Secs. IV and V. This work is concluded in Sec. VI.

II. EXPERIMENTAL DETAILS

Measurements were conducted in a low-speed, closed-circuit wind tunnel with a 2.4-m-long square test section of 0.6×0.6 m^2. The nonuniformity of the flow in the test section was 0.5% and the turbulent intensity was less than 0.4% for the present U_∞ examined. U_∞ was measured using a Pitot-static tube connected to a Furness micromanometer, with an uncertainty of less than 2.0%. More details of the tunnel were given by Huang *et al.*[16]

Two brass cylinders of the same diameter, $d=12.5$ mm, were used as the test models, spanned the full width of the working section, and mounted symmetrically with respect to the middle plane, 0.2 m downstream of the exit plane of the contraction section of the wind tunnel. The total geometric blockage of the two cylinders was 4.2%, less than the level (6%) that may affect the flow appreciably.[17] The length-to-diameter ratio of the cylinder was 48. Figure 1(a) shows the arrangement of the cylinders and the definitions of P and α. The Cartesian coordinate system was defined such that the origin was at the midpoint between the two cylinders, with the x- and y-axes along the flow and the transverse directions, respectively.

Two single hotwires (Pt-10% Rh) of 5 μm in diameter and about 1 mm in length were placed symmetrically with respect to the x-axis at $x/d=5.0$ and $y/d=\pm(0.5P^*\sin\alpha+1)$ to measure simultaneously the streamwise velocity fluctuation u behind each of the two cylinders. The choice of y/d ensured that one hotwire was located $1.0d$ below the center of the lower cylinder and the other $1.0d$ above that of the upper cylinder, that is, both wires were placed on the free-stream side of the cylinders. The power spectral density function of the u signal measured at $x/d=2.5-10.0$ and $y/d=-3-3$ by Hu and Zhou[9] could display multiple pro-

Downloaded 17 Mar 2011 to 158.132.161.180. Redistribution subject to AIP license or copyright; see http://pof.aip.org/about/rights_and_permissions

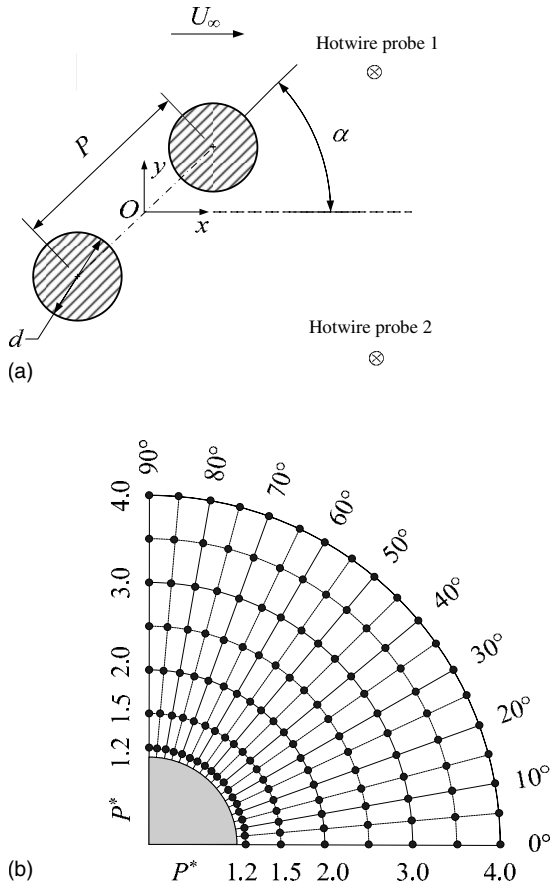

FIG. 1. (a) Experimental arrangement; (b) hotwire measurement grid in the P^*-α plane.

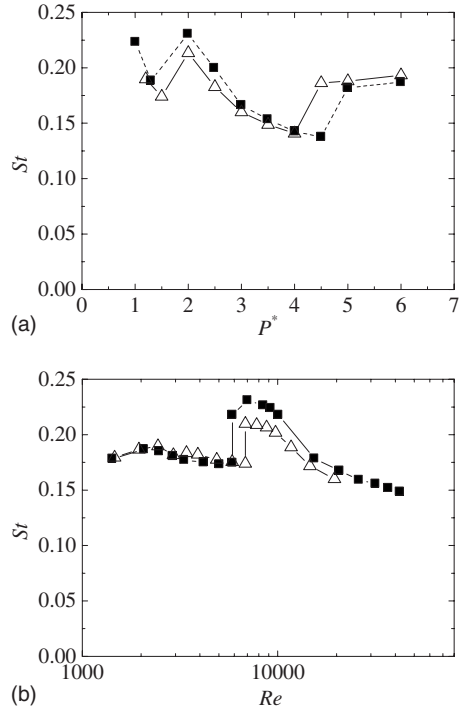

FIG. 2. Comparison between the measured St and that of Xu and Zhou (Ref. 13) at $\alpha=0°$: (a) the dependence of St on P^* (Re=7000); (b) the dependence of St on Re at $P^*=2.0$. (△) Present; (■) Xu and Zhou (Ref. 13).

nounced peaks at $x/d=2.5$ because of vigorous interaction between the upstream- and downstream-cylinder-generated vortices, which can be confusing in determining St. This confusion is alleviated with the wires placed at $x/d=5.0$. Similar consideration was given in determining the transverse location of the wires. The hotwires were operated at an overheating ratio of 1.8 on a constant temperature circuit. The hotwire signals were low-pass filtered (with a cutoff frequency of 1.0 kHz), offset, amplified, and then digitized using a 16 channel (12 bits) A/D board at a sampling frequency of 2.5 kHz. The duration of each signal was 20 s. No calibration was performed. The power spectral density function E_u of u was calculated using a fast Fourier transform, with a frequency resolution of about 0.854 Hz. The corresponding maximum error in the estimated St was about $\pm 1.0\%$. The Re range investigated is $(1.5\times10^3)-(2.0\times10^4)$. The configuration of the cylinders covers $\alpha=0°-90°$ and $P^*=1.2$, 1.5, 2.0, 2.5, 3.0, and 4.0 for the entire Re range. The increment $\Delta\alpha$ was 10° but was reduced to 5° for $\mathrm{Re}=1.5\times10^3$, 7.0×10^3, and 2.0×10^4.

III. CONFIGURATIONS OF $\alpha=0°$ AND 90°: VALIDATION OF MEASUREMENTS

The St data in the wake of two tandem cylinders have been well documented in literature. Similarly, there have been a number of previous reports on the St data for the side-by-side-arranged cylinders. Therefore, the data from the two special configurations are used as a reference for the validation of the present measurement. Figure 2(a) shows reasonable agreement between the presently measured St dependence on P^* at $\alpha=0°$ and that of the same Re ($\mathrm{Re}=7.0\times10^3$), as reported by Xu and Zhou.[13] The two rapid rises in St, one from $P^*\approx1.3$ to 2 and the other from $P^*\approx4$ to 5, correspond to the occurrence of two bistable phenomena. The latter results from a transition of the shear layer, separating from the upstream cylinder, from the reattachment to the coshedding regime.[5,10,12,18] The present critical P^*, between 4.0 and 4.5, is slightly smaller than the measurements of Xu and Zhou.[13] The deviation is not unexpected. The occurrence of the critical P^*, usually between 3.0 and 5.0, is highly dependent on Re, turbulence intensity, cylinder aspect ratio, blockage ratio, cylinder-surface roughness, etc.[13,18] The blockage and aspect ratios are presently 2.1% and 48, respectively, and 2.5% and 40, respectively, in the measurements of Xu and Zhou. Furthermore, the relatively large increment, $\Delta P^*=0.5$, and uncertainties in determining P^* and α also contribute to the deviation. The rapid rise in St between $P^*=1.3$ and 2 is ascribed to a transition from shear layer rollup behind the downstream cylinder to reattachment on the downstream side of the cylinder.[13] The monotonic decrease in St from $P^*=2$ to 4 results from a shift in the reattachment position toward the forward stagnation point.

Figure 2(b) compares the presently measured dependence of St on Re at $P^*=2.0$, which is in the reattachment regime, with the data of Xu and Zhou.[13] The agreement between the two measurements is, in general, quite good. Both measurements display a sudden jump in St, which is again ascribed to a transition from shear layer rollup behind to reattachment on the downstream side of the downstream cyl-

Downloaded 17 Mar 2011 to 158.132.161.180. Redistribution subject to AIP license or copyright; see http://pof.aip.org/about/rights_and_permissions

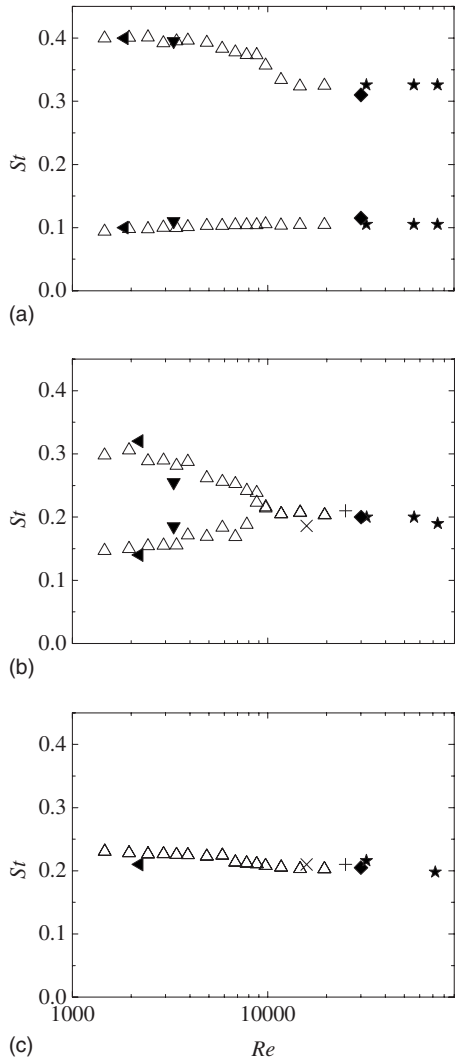

FIG. 3. Comparison between the measured St and the data available in literature at $\alpha=90°$. (a) $P^*=1.5$; (b) 2.0; (c) 3.0. (△) Present; (×) Ref. 4; (▼) Ref. 14; (◀) Ref. 19; (★) Ref. 20; (♦) Ref. 21; (+) Ref. 22.

inder. The same explanation for the discrepancy in Fig. 2(a) may apply for the small departure of the present data from the measurements of Xu and Zhou,[13] in particular, at the Re range beyond the sudden jump.

The presently obtained St-Re relationship for the side-by-side-arranged cylinders is compared to previous measurements at $P^*=1.5$, 2.0, and 3.0, which are available only for a limited number of Re. The case of $P^*=1.5$ corresponds to the asymmetric flow regime throughout the Re range presently examined. In this regime, the flow is characterized by one narrow and one wide wake associated with a high and a low St [Fig. 3(a)], respectively.[5,15,19,23] Two distinct values of St are observed [Fig. 3(a)]. The lower St is close to 0.1, displaying little variation with Re. However, the dependence of the higher St on Re is rather appreciable; St is close to 0.4 between 1.5×10^3 and 5.0×10^3 but decreases gradually to 0.33 at $\mathrm{Re}=1.2\times10^4$. With Re increasing further, St remains almost constant up to $\mathrm{Re}=7.4\times10^4$. At $P^*=2.0$, two distinct St values occur for $\mathrm{Re}<1.0\times10^4$ [Fig. 3(b)] but merge into one, about 0.2, for higher Re, the same as St_0. The following observations can be made. (i) As Re increases, the asymmetric (flip-flopping) flow occurs at $\mathrm{Re}<1.0\times10^4$ and changes to two symmetrically or antisymmetrically arranged vortex streets at $\mathrm{Re}=1.0\times10^4$. (ii) At $\mathrm{Re}=1.0\times10^4$, with increasing P^*, the asymmetric flow will be altered to a symmetric or antisymmetric flow at a critical $P^*(\approx2.0)$. (iii) This critical P^* is smaller at higher Re. At $P^*=3.0$, a single St is detected throughout the ranges of Re examined [Fig. 3(c)]. As Re increases, St drops slowly up to $\mathrm{Re}=1.0\times10^4$ and remains almost constant for $\mathrm{Re}>1.0\times10^4$. The observation is rather similar to an isolated cylinder wake, where St_0 decreases with increasing Re in the lower subcritical range [$\mathrm{Re}=(2.0\times10^3)-(1.0\times10^4)$] and remains almost unchanged in the higher subcritical range, i.e., $\mathrm{Re}=(1.0\times10^4)-(2.0\times10^5)$.[24,25] The agreement between present and previous data provides a validation for the present measurement.

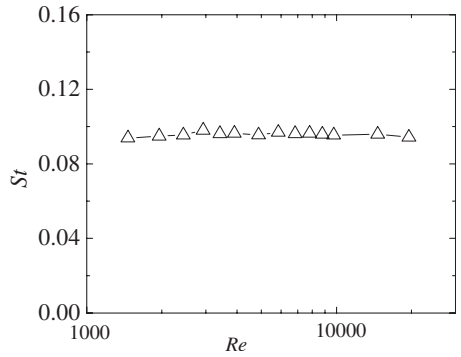

FIG. 4. The St-Re relationship of type 1, characterized by a single St. $P^*=1.2$ and $\alpha=90°$.

IV. CLASSIFICATION OF THE St-Re RELATIONSHIPS

For each measurement point in the P^*-α plane [Fig. 1(b)], St at each Re is determined from E_u and a St-Re correlation is obtained from $\mathrm{Re}=1.5\times10^3$ to 2.0×10^4. After careful examination, these plots, altogether 70, are classified into four types, i.e., types 1–4. Each type is discussed below.

A. Type 1

This type of the St-Re relationship is a near constant single St over the Re range examined (Fig. 4). The corresponding P^* is small, not exceeding 1.1–1.25, the exact value depending on α. As such, the two cylinders behave as a single body, producing a single street and corresponding to the flow structure of S-I.[6] The typical E_u (Fig. 5) displays one pronounced peak at St=0.09. If normalized on the actual or effective bluff width ($\sim2.2d$), St would be 0.198, essentially the same as St_0. A minor peak is discernible at St=0.19 in both spectra, probably arising from the second harmonic of 0.09.

Type 1 may have four distinct interactions of shear layers around the cylinders, as schematically shown in Figs. 6(a)–6(d), based on the data in literature and our present measurements. At $P^*=1.0$, there is no flow through the gap [Fig. 6(a)], and the flow structure results essentially from the rollup of the two outer shear layers, as behind an isolated cylinder. At $P^*<1.1-1.2$ and $\alpha>20°$, the gap flow pen-

Downloaded 17 Mar 2011 to 158.132.161.180. Redistribution subject to AIP license or copyright; see http://pof.aip.org/about/rights_and_permissions

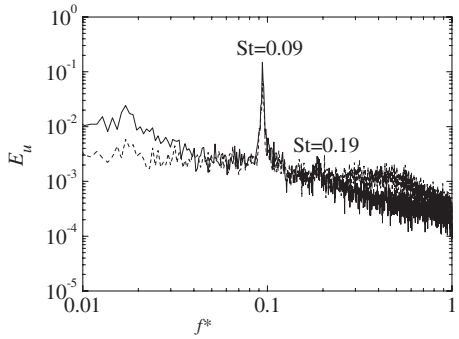

FIG. 5. Typical power spectral density functions for the St-Re relationship of type 1. $P^*=1.2$, $\alpha=90°$, and $\mathrm{Re}=7.0\times10^3$. (Solid line) Downstream cylinder (probe 1); (dashed line) upstream cylinder (probe 2).

etrates into the base region of the upstream cylinder [Fig. 6(b)] although slowed because of the near-wall friction force, producing very small-scaled or no vortices and adding extra turbulence in the wake. This bleeding acts to prolong the vortex formation region.[19,23] Nevertheless, its influence is weak and the outer shear layers largely dictate the formation of the flow structure. St changes little with increasing Re (Fig. 4) because the gap-flow-added turbulence in the wake overwhelms the turbulence added in the shear layers or wake due to an increase in Re. The two flow structures in Figs. 6(a) and 6(b) were reported by Sumner *et al.*[2] At $0°<\alpha<20°$, the downstream cylinder cuts in the upstream cylinder wake, and flow through the gap may be substantially weakened [Fig. 6(c)]. The inner shear layer separating from the upstream cylinder reattaches on the downstream cylinder and bifurcates [Fig. 6(c)]. Due to a small P^*, part of the bifurcated flow may bounce back to the upstream cylinder, forming a separation bubble on the upstream cylinder.[26] The bubble has a great impact on the upstream cylinder lift but not on St (Refs. 8 and 26) as the outer shear layers of the two cylinders alternately form vortices. At $\alpha\approx0°$, the two shear layers separating from the upstream cylinder overshoot the downstream cylinder, generating a staggered vortex street [Fig. 6(d)].

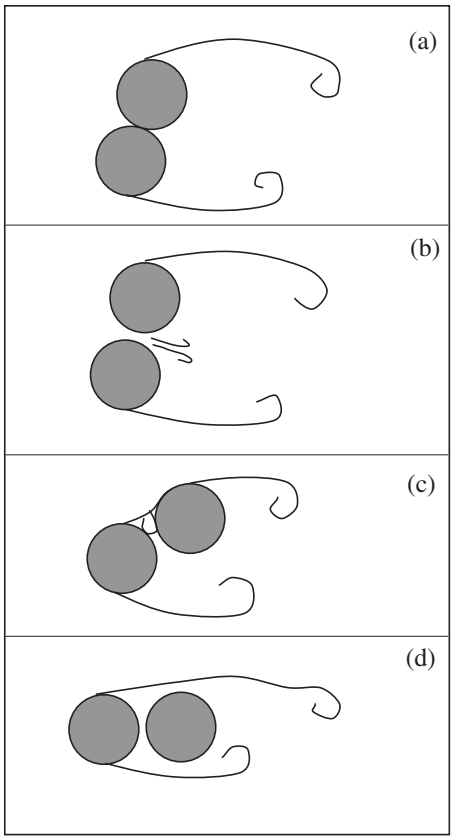

FIG. 6. Schematic of typical flow structures associated with type 1. The Re effect on the flow structure is insignificant. Flow is left to right.

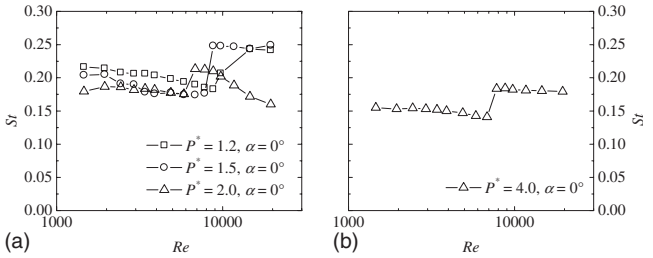

FIG. 7. The St-Re relationship of type 2, characterized by a sudden jump in St: (a) type 2A, where the jump is attributed to a change from the single-body-like to the reattachment regime; (b) type 2B, where the jump results from a change from the reattachment to the coshedding regime.

B. Type 2

Type 2 occurs at small α, not exceeding 10°, and $P^*=1.2-4.0$, which corresponds approximately to the flow regime of S-Ib.[6] Although again single valued, St displays a sudden jump at $\mathrm{Re}=(6.5\times10^3)-(1.0\times10^4)$ (Fig. 7), depending on P^*. Based on mechanisms responsible for the jump, type 2 is further divided into subtypes 2A and 2B. Figure 8 illustrates typical E_u at Re before and after the jump. For type 2A [Fig. 8(a)], St is 0.17 at $\mathrm{Re}=4.0\times10^3$ but 0.24 at $\mathrm{Re}=1.0\times10^4$, below and beyond St_0, respectively. The presence of other small peaks at $\mathrm{Re}=1.0\times10^4$ may be a signature of unstable shear-layer reattachment on the downstream side of the cylinder. For type 2B, St is 0.15 at $\mathrm{Re}=4.0\times10^3$ [Fig. 8(b)] and rises to 0.18, close to St_0, at $\mathrm{Re}=1.2\times10^4$. Alam and Zhou[27] observed at $\mathrm{Re}=2.72\times10^4$ two St behind the downstream cylinder at $P^*=6$ and $\alpha=0°$ (the coshedding flow regime). One was identical to the frequency of vortex shedding from the upstream cylinder, and the other, corresponding to a rather minor peak in E_u, was ascribed to vortex shedding from the downstream cylinder. They failed to detect the latter when placing the hotwire probe appreciably away from the centerline, which probably explains why one St only is observed presently (the hotwire was placed at $y^*=1.0$).

Type 2A occurs at $1.1<P^*\leq2.5$ [Fig. 7(a)]. The critical Reynolds number (Re_c), at which the jump in St occurs, decreases with increasing P^*; for example, Re_c is 9.5×10^3, 8.5×10^3, and 6.5×10^3 at $P^*=1.2$, 1.5, and 2.0, respectively. At $\mathrm{Re}<\mathrm{Re}_c$, the shear layers separating from the upstream cylinder shoot over the downstream one [Fig. 9(a)] and the two cylinders act like a single body, with stagnant fluid in their gap.[5,10] This explains why St is close to St_0. For $\mathrm{Re}<\mathrm{Re}_c$, St at a given P^* drops slowly and monotonically with

Downloaded 17 Mar 2011 to 158.132.161.180. Redistribution subject to AIP license or copyright; see http://pof.aip.org/about/rights_and_permissions

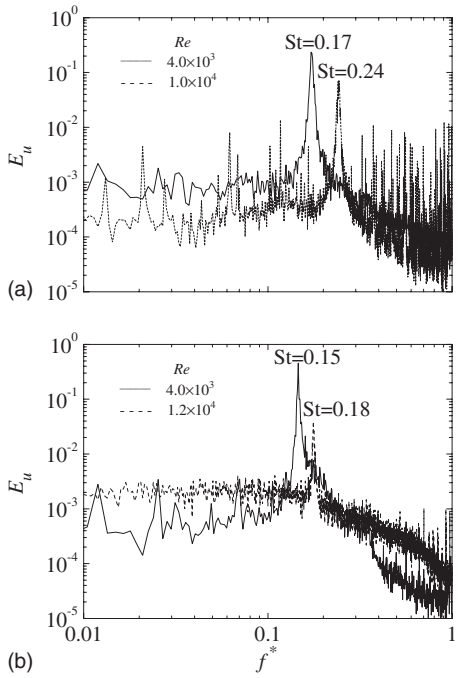

FIG. 8. Typical power spectral density functions, E_u, for the Re-St relationship of type 2. (a) Type 2A: $P^*=1.5$ and $\alpha=0°$. (b) Type 2B: $P^*=4.0$ and $\alpha=0°$. Being essentially the same from both probes, E_u, from probe 1 only is presented.

increasing Re, which is attributed to a decrease in the vortex formation length. In a single cylinder wake, the formation length reduces rapidly from $2.7d$ at $\mathrm{Re}=10^3$ to $1.5d$ at $\mathrm{Re}=10^4$ and remains unchanged up to 2.0×10^5.[18] A shorter length corresponds to a lower St and vice versa.[25,28,29] Since the formation length of type 2A retreats with increasing Re, the rollup of the overshooting shear layers [Fig. 9(a)] occurs near and eventually reattaches on the downstream cylinder [Fig. 9(b)],[30] producing a jump in St at $\mathrm{Re}=\mathrm{Re}_c$. Given Re ($\mathrm{Re}<\mathrm{Re}_c$), an increased P^* results in a slight decrease in St. Since the downstream cylinder is completely submerged in the recirculation region of the upstream cylinder wake, a larger P^* implies a longer after-body length of the combined body and hence a reduced St. The St dependence on P^* resembles that on the width-to-height ratio (an indication of after-body length) in a rectangular cylinder wake, where St diminishes gradually as the width-to-height ratio increases up to 2.8.[31–33]

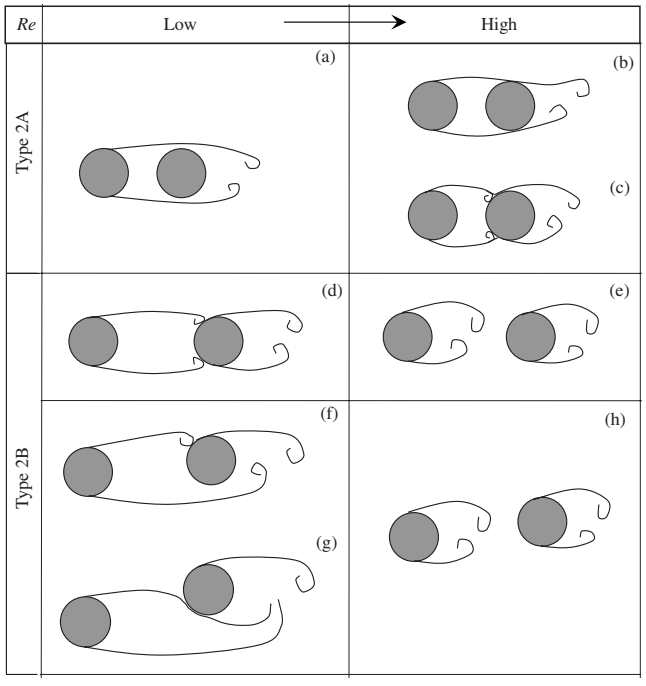

FIG. 9. Schematic of typical flow structures associated with type 2. With increasing Re, flows in the left column change to those in the right. (a) Overshooting flow, [(b)–(d), (f), and (g)] shear-layer-reattachment flow, and [(e) and (h)] coshedding flow. Flow is left to right.

For $\mathrm{Re}>\mathrm{Re}_c$, the shear layer reattachment results in a narrowed wake behind the downstream cylinder and hence a higher St, which is highly dependent on the reattachment location on the downstream cylinder.[34] A shear layer reattaching on the downstream side of the cylinder is led toward the centerline [Fig. 9(b)], producing a narrowed wake and hence an increased St. Expectedly, at $P^*=1.2$ and 1.5, reattachment occurs on the downstream side for $\mathrm{Re}>\mathrm{Re}_c$. On the other hand, a shear layer reattaching on the upstream side is diverted away from the centerline, resulting in a wider wake and a lower St. At $P^*=2.0$, St is smaller than at $P^*=1.2$ and 1.5 [Fig. 7(a)], and reattachment occurs probably at $\theta\approx90°$ for $\mathrm{Re}=(6.5–8.5)\times10^3$, over which St is almost constant, and on the upstream side for $\mathrm{Re}>8.5\times10^3$ [Fig. 9(c)], where St drops with increasing Re due to a shift of reattachment further upstream.

Note that a smaller P^* implies that the downstream cylinder, submerged in the recirculation region of the upstream-cylinder wake, may be further separated from the rollup of the shear layers, that is, a greater increase in Re is required to achieve adequate reduction in the formation length and hence to cause the occurrence of reattachment. This explains the observation that a smaller P^* corresponds to a higher Re_c.

Type 2B occurs at larger P^*, in the range of 2.5–4 [Fig. 7(b)]; the values of St are between 0.14 and 0.16 for $\mathrm{Re}<\mathrm{Re}_c$ ($=7.5\times10^3$) and 0.185 for $\mathrm{Re}>\mathrm{Re}_c$. In the reattachment regime ($\mathrm{Re}<\mathrm{Re}_c$), the shear layers reattach on the upstream side of the downstream cylinder, resulting in St values considerably smaller than St_0. It is noteworthy that St at $\mathrm{Re}<\mathrm{Re}_c$ [Fig. 7(b)] is almost the same as at $P^*=2.0$ and $\mathrm{Re}=2\times10^4$ [Fig. 7(a)] perhaps because reattachment occurs on the upstream side of the cylinder for both cases [Figs. 9(c) and 9(d)]. The shrinking St values, although slowly, from $\mathrm{Re}=1.5\times10^3$ to Re_c, are attributed to an upstream shift of the reattachment position on the downstream cylinder. The movement of the reattachment position is linked to a reduction in the vortex formation length of the upstream cylinder wake in the absence of the downstream cylinder. Beyond Re_c both cylinders generate vortices. Vortex shedding from the downstream cylinder is triggered by that from the upstream cylinder,[12,13,27,34] thus resulting in the same St behind each cylinder, which is close to St_0.

Four distinct interactions between the shear layers around the two cylinders are possible in type 2 and may change from one to another with increasing Re: (1) both shear layers, separating from the upstream cylinder, over-

Downloaded 17 Mar 2011 to 158.132.161.180. Redistribution subject to AIP license or copyright; see http://pof.aip.org/about/rights_and_permissions

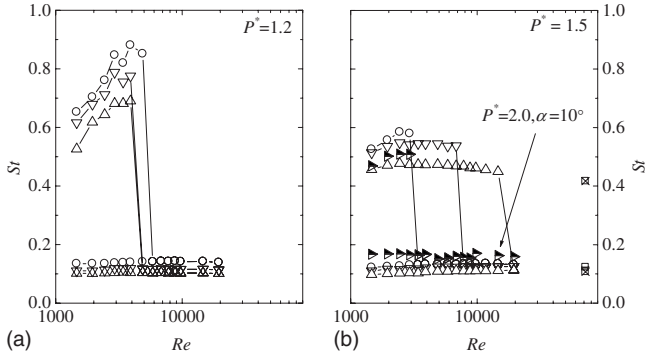

FIG. 10. The St-Re relationship of type 3, characterized by the occurrence of two distinct St. (a) $P^*=1.2$; (b) 1.5, 2.0. Present data: (○) $\alpha=30°$; (▽) 50°; (△) 70°.

shooting the downstream cylinder [Fig. 9(a)]; (2) both reattaching [Figs. 9(b)–9(d)]; (3) one overshooting and the other reattaching [Figs. 9(f) and 9(g)]; (4) both rolling up to form staggered vortices before reaching the downstream cylinder [Figs. 9(e) and 9(h)]. Scenario (1) occurs in type 2A and small Re, and changes to (2) with increasing Re. Scenarios (2) and (3) occur in type 2B. At $\alpha\approx 0°$, both shear layers reattach symmetrically on the upstream side of the downstream cylinder [scenario (2), Fig. 9(d)]. At $0°<\alpha<5°$, since the downstream cylinder is placed away from the wake centerline, only the inner shear layer reattaches on the outer side of the downstream cylinder [scenario (3), Fig. 9(f)]. At $5°<\alpha<10°$, reattachment occurs near or below the nominal stagnation point, with the reattached shear layer diverted along the lower side of the downstream cylinder [Fig. 9(g)]. They all change to scenario (4) with increasing Re.

C. Type 3

In the intermediate range of P^* and α, i.e., $P^*=(1.1-1.2)-(1.5-2.2)$ and $\alpha=10°-75°$, the St-Re relationship, referred to as type 3, is characterized by two distinct values of St at low Re, but the higher St will suddenly collapse to the lower St with increasing Re [Figs. 10(a) and 10(b)]. The value of Re_c, at which the sudden collapse occurs, varies from 3.5×10^3 to 2.0×10^4; a smaller α and/or smaller P^* corresponds to a smaller Re_c. The lower value of St is insensitive to Re and occurs, depending on α, between 0.1 and 0.15, considerably smaller than St_0. The higher St grows with Re at $P^*<1.4$ [Fig. 10(a)] but remains more or less constant at $P^*>1.4$ [Fig. 10(b)]. Its value exceeds 0.42, reaching 0.88 at $\alpha=30°$ and $\mathrm{Re}=4.0\times10^3$ ($P^*=1.2$), slightly more than that (0.84) observed by Ishigai *et al.*[35] at $\alpha=25°$ and $P^*=1.12$ ($\mathrm{Re}\approx5.0\times10^3$). One may suspect whether such a high St originates from the shear layer instability, instead of Karman vortices. The peak, corresponding to the shear layer instability, is usually broadbanded in the power spectral density function of fluctuating velocities.[13,36] However, a sharp peak occurs presently at the high St [Fig. 11(a), $P^*=1.2$]. The typical E_u, measured in either wakes, displays two pronounced peaks at St=0.11 and 0.69 at $\mathrm{Re}=2.5\times10^3$ [Fig. 11(a)] and a single peak at St=0.11 at $\mathrm{Re}=1.0\times10^4$ [Fig. 11(b)], where the higher St vanishes. Two minor

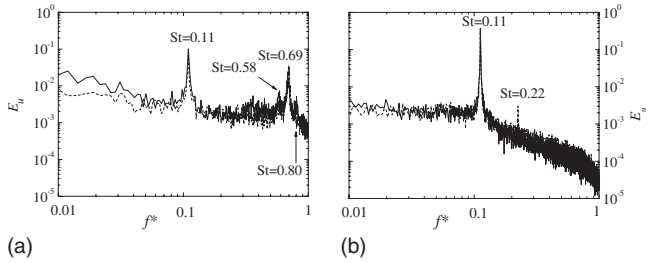

FIG. 11. Typical power spectral density functions for the St-Re relationship of type 3. $P^*=1.2$ and $\alpha=50°$: (a) $\mathrm{Re}=2.5\times10^3$ and (b) 1.0×10^4. (Solid line) Downstream cylinder (probe 1); (dashed line) upstream cylinder (probe 2).

peaks occur at $f^*=0.58$ and 0.80 in E_u [Fig. 11(a)] measured in the downstream cylinder wake, which result from the addition and subtraction of St=0.11 and 0.69, respectively. Based on flow visualization at low Re (820–1900), Sumner *et al.*[2] observed at $P^*=1.5$ two St, 0.52 and 0.12 for $\alpha=25°-35°$ and 0.48 and 0.11 for $\alpha=55°-65°$, which were connected to a vortex-pairing-enveloping flow and a vortex-pairing-splitting-enveloping flow, respectively. The present higher value of St at Re=1500 is about 0.52–0.62 ($\alpha=30°-70°$) and grows with increasing Re [Fig. 10(a)]. It is therefore speculated that the higher value of St in Figs. 10(a) and 10(b) may be connected to the vortex-pairing-enveloping or vortex-pairing-splitting-enveloping flow.

At low Re, the shear layers on either side of the gap form two synchronized opposite-signed vortices [Figs. 12(a) and 12(c)]. The two may pair during their downstream evolution. The upstream and downstream cylinders produce a narrow and a wide wake, respectively. The outer shear layer of the upstream cylinder forms the vortices of the same frequency as those in the gap.[2,8] This frequency is much higher than that of vortices shed from the outer side of the downstream cylinder. Thus, two distinct values of St occur. The gap vortices have a higher streamwise velocity because of the jet-like flow through the gap and the pairing of two oppositely signed vortices, which enhances the streamwise velocity significantly.[37] The increased velocity may enable the paired vortex to approach the vortex produced from the outer shear layer of the upstream cylinder, producing a favorable condition for the paired vortex to be enveloped. At small P^*

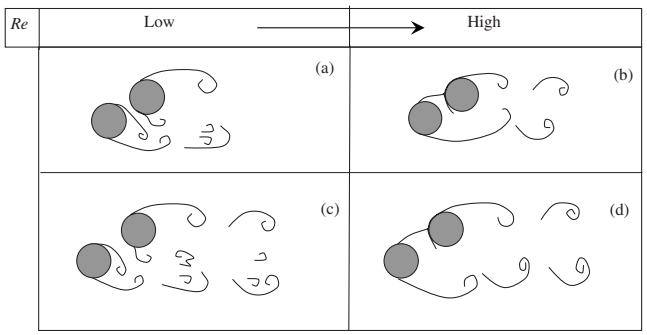

FIG. 12. Schematic of typical flow structures associated with type 3. With increasing Re, flows in the left column changes to those in the right. (a) Vortex-pairing-enveloping flow, [(b) and (d)] shear-layer-reattachment flow, and (c) vortex-pairing-splitting-enveloping flow. Flow is left to right.

Downloaded 17 Mar 2011 to 158.132.161.180. Redistribution subject to AIP license or copyright; see http://pof.aip.org/about/rights_and_permissions

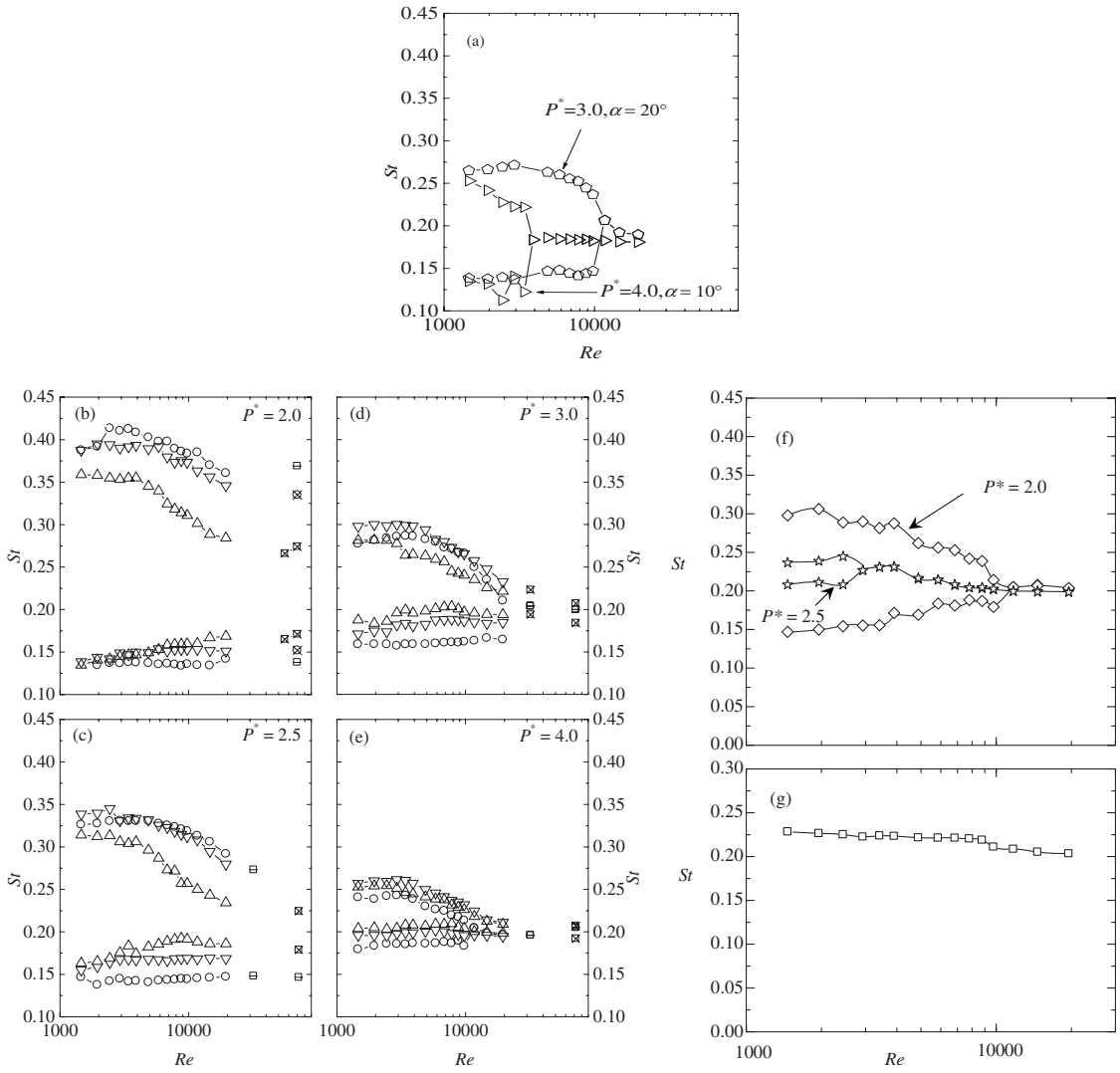

FIG. 13. The St-Re relationship of type 4. (a) Type 4A: $P^*=3.0$ ($\alpha=20°$) and 4.0 ($\alpha=10°$). [(b)–(e)] Type 4B: present data: (○) $\alpha=30°$; (▽) 50°; (△) 70°. By Sumner *et al.* (2005) (⊟) 30°; (⊗) 50°; (⊠) 70°; (⊖) 90°. (f) Type 4C: $P^*=2.0$ and 2.5 ($\alpha=90°$). (g) Type 4D: $P^*=4.0$ ($\alpha=90°$).

(<1.4), the gap flow is very narrow, and the pairing vortices are close to each other, thus completely enveloped by the relatively large vortex originating from the outer shear layer of the upstream cylinder [Fig. 12(a)]. At relatively large P^*, flow through the gap is enlarged laterally and the pairing vortices are increased in size, not so close to each other. As a result, the vortex from the outer shear layer could not envelop both but only a fraction of the pair [Fig. 12(c)]. See Ref. 2 at $P^*=1.5$ and $\alpha=60°$ for examples. The flow is characterized by the gap vortex pairing enveloping. The flows in Figs. 12(a) and 12(c) are characterized by a narrow and a wide jet-like gap flow, respectively. Accordingly, the former has a very high value of St (0.55–0.88) and the latter a moderately high value of St (0.4–0.55) [Figs. 10(a) and 10(b)].

One may wonder what happens with the flow so that the higher value of St that occurred at low Re ($<\mathrm{Re}_c$) suddenly collapses to the lower. It is well known that at a moderate P^*, the downstream cylinder acts to divert the gap flow toward the wake centerline of the upstream cylinder, resulting in the wide wake of lower St behind the downstream cylinder and a narrow wake of higher St behind the upstream cylinder.[2,4,5,20,26] For the present Re range, the boundary layer over the upstream cylinder becomes thinner with increasing Re and the separation point shifts upstream toward the forward stagnation point,[25] implying an increased separation angle. With an adequate upstream shift at $\mathrm{Re}>\mathrm{Re}_c$, the inner shear layer, separated from the upstream cylinder, reattaches on the downstream cylinder; part of it separates from the gap side, generating a shear-layer-reattachment flow that forms a small gap flow [Fig. 12(b)]. As a result, the higher St disappears; the two outer shear layers, separated from the two cylinders, form vortices alternately at the lower St.

D. Type 4

Type 4 corresponds in general to a larger value of P^* than type 3. Two distinct St values occur at low Re but change into or approach a single and intermediate value with increasing Re. Based on flow physics behind the change, type 4 was further divided into type 4A [Fig. 13(a)], type 4B [Figs. 13(b)–13(e)], type 4C [Fig. 13(f)], and type 4D [Fig. 13(g)].

Type 4A occurs at a relatively small α (α

Downloaded 17 Mar 2011 to 158.132.161.180. Redistribution subject to AIP license or copyright; see http://pof.aip.org/about/rights_and_permissions

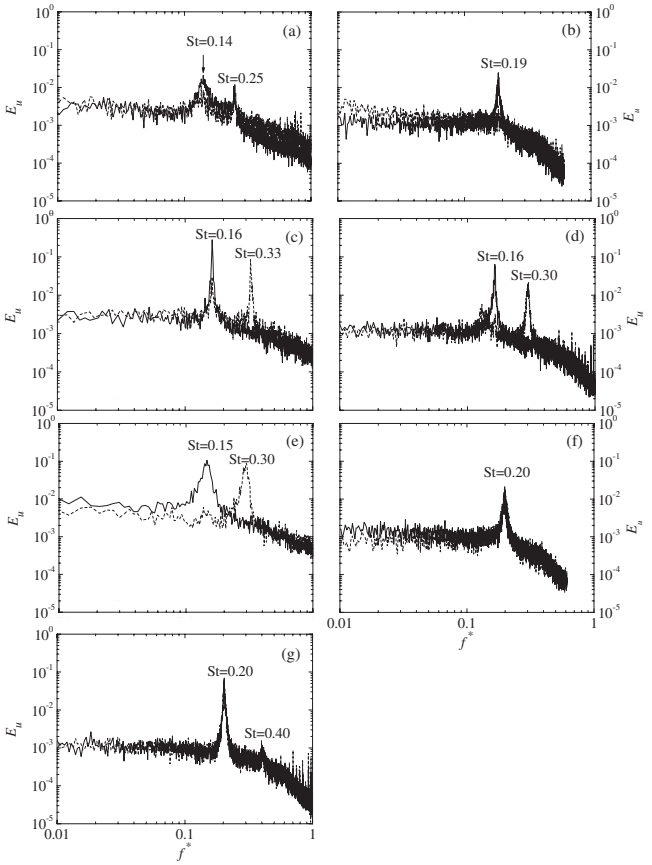

FIG. 14. Typical power spectral density functions for the St-Re relationship of type 4. Type 4A ($P^*=3.0$, $\alpha=20°$): (a) $Re=7.0\times10^3$ and (b) 2.0×10^4. Type 4B (2.5, 50°): (c) 4.0×10^3 and (d) 1.2×10^4. Type 4C (2.0, 90°): (e) 2.0×10^3 and (f) 2.0×10^4. Type 4D (4.0, 90°): (g) 1.2×10^4). (Solid line) Downstream cylinder (probe 1); (dashed line) upstream cylinder (probe 2).

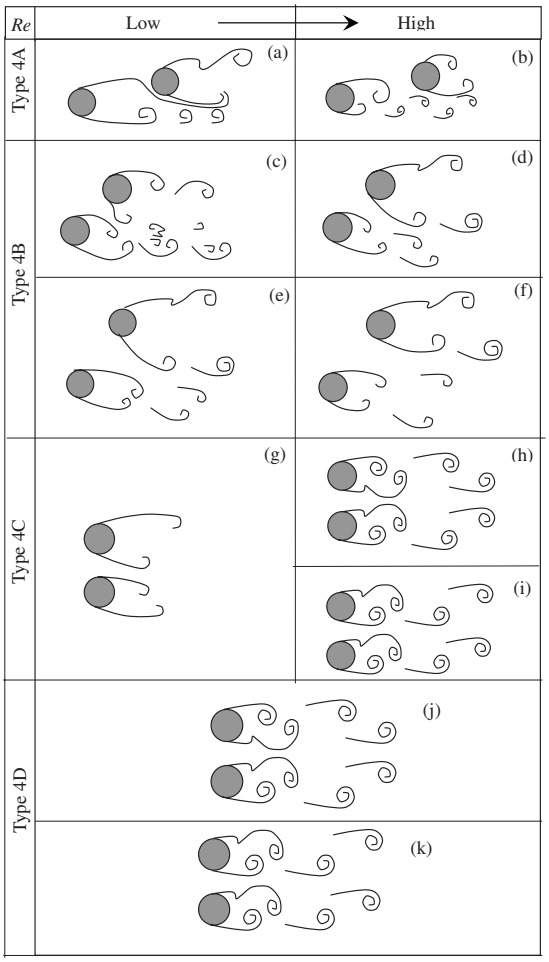

FIG. 15. Schematic of typical flow structures associated with type 4. With increasing Re, flows in the left column changes to those in the right. Type 4D is insensitive of Re. (a) Induced separation flow, (b) coshedding flow, (c) vortex-pairing-splitting-enveloping flow, [(d)–(g)] no-enveloping flow, [(h)–(k)] coupled vortex-shedding flow in [(h) and (j)] antiphased and [(j) and (k)] in-phased arrangements. Flow is left to right.

$=10°-20°$, $P^*=2.2-4$). At low Re, both E_u in Fig. 14(a) display two peaks, resembling qualitatively that of type 3 [Fig. 11(a)] although the higher St value in type 4A is considerably smaller than that in type 3. When the downstream cylinder is displaced from the centerline of the upstream cylinder wake, the shear layer separating from the inner side of the upstream cylinder runs toward and dives beneath the downstream cylinder without reattachment [Fig. 15(a)]. The outer shear layer separated from the upstream cylinder forms vortices at the higher St, while the shear layers over the downstream cylinder form vortices at the lower St.[2,8,26] As advected downstream, the vortices of the higher value of St interact with those of the lower St, producing a single combined street of the lower St. Since the vortex formation length reduces from $Re=3.0\times10^3$ to 2×10^4, the shear layer separated from the inner side of the upstream cylinder may roll up to form vortices before reaching the downstream cylinder, producing a coshedding flow [Fig. 15(b)]. As such, the upstream cylinder wake displays similarity to that behind an isolated cylinder. Meanwhile, vortex shedding from the downstream cylinder is triggered by the vortices separated from the inner side of the upstream cylinder. The change from the flow shown in Fig. 15(a) to the other [Fig. 15(b)] is discontinuous,[13,26] resulting in the rather abrupt collapse of the two St values into about 0.19 [Fig. 14(b)].

Type 4B occurs at a larger value of α ($20°<\alpha<88°$, $P^*>1.2-2.2$) than type 4A. Unlike type 4A, there is no sudden change in St with increasing Re for type 4B. At $P^*\leq2.5$, the downstream cylinder pushes the gap flow toward the centerline of the upstream cylinder wake [Figs. 15(c) and 15(e)], generating a narrow wake of higher St behind the upstream cylinder and a wide wake of lower St behind the downstream cylinder. The higher St varies little for $Re=(1.5-3)\times10^3$ but declines rather rapidly from $Re=3\times10^3$ to 2×10^4 [Figs. 13(b)–13(e)]. Meanwhile, the lower St rises, although slowly. The upstream cylinder is subjected to a uniform incident flow, but the downstream cylinder is not. Naturally, the Re effect on the narrow wake is significant and may behave similarly to an isolated cylinder wake, where St is almost constant for $Re=(6\times10^2)-(3\times10^3)$ but reduces considerably from $Re=3\times10^3$ to 2×10^4.[25,38–40] The St behavior is linked to the vortex formation length, which is insensitive for $Re=(6\times10^2)-(3\times10^3)$ but shrinks exponentially from $Re=3\times10^3$ to 2×10^4.[28,41,42] Given an exponentially reducing vortex formation length associated with the upstream cylinder for Re

Downloaded 17 Mar 2011 to 158.132.161.180. Redistribution subject to AIP license or copyright; see http://pof.aip.org/about/rights_and_permissions

$=(3.0\times10^3)-(2\times10^4)$, the flow around the downstream cylinder should be less affected by the upstream cylinder and behave more like an isolated cylinder wake. Therefore, the St values associated with the downstream and upstream cylinders grow and decline, respectively, both approaching St_0; their difference is larger at smaller P^* and/or α, where the interactions between the two wakes is more intensified. As P^* increases (>2.5), the flow structure at low Re [Fig. 15(e)] is similar to that of $P^*\leq2.5$ at higher Re [Fig. 15(d)], i.e., no-enveloping flow, as corroborated by the St value, which is almost the same at $Re\approx2\times10^4$ [Figs. 13(b) and 13(c)], and at $Re<2\times10^3$ [Figs. 13(d) and 13(e)]. With increasing Re, the two streets tend to interact less intensively [Fig. 15(f)], their St values approaching St_0 [Figs. 13(d) and 13(e)].

As shown in E_u (Fig. 14), the St value measured behind the downstream cylinder is 0.16 and that behind the upstream cylinder is 0.33 at $Re=4.0\times10^3$ [Fig. 14(c)]. Due to relatively large P^* and α, the downstream-cylinder-generated wake is wide enough so that the hotwire placed in it failed to capture the higher value of St [Fig. 14(c)]. As Re increases to $Re=1.2\times10^4$, the hotwire placed behind the upstream cylinder failed to capture the lower St and the peak corresponding to the higher St in E_u is less pronounced [Fig. 14(d)], consistent with the occurrence of the no-enveloping flow [Figs. 15(d) and 15(f)].

The data of Sumner *et al.*[20] is inserted in Figs. 13(b)–13(e) to extend the Re range examined beyond $Re=2\times10^4$. The value of St at $Re=2\times10^4$ is, in general, very close to that at $Re=2.0\times10^4$ of the same P^* and α, suggesting that the Re effect on St, although significant for $Re<2.0\times10^4$, is small for $Re>2.0\times10^4$. The insignificant Re effect is connected to the fact that the vortex formation length in an isolated cylinder wake is insensitive to Re for $Re=(2.0\times10^4)-(2.0\times10^5)$.[12,28,43]

Type 4C corresponds to the regions of $\alpha=88°-90°$ and $P^*=1.7-2.7$, where the gap flow is biased at low Re, producing a narrow street of higher St and a wide street of lower St. With increasing Re, the two distinct St values approach each other and eventually meet at $St\approx0.2$ [Fig. 13(f)], which implies that the gap flow is not biased any more and two antiphased streets of the same St occur, each similar to that behind an isolated cylinder. It is well known that in the wake of two side-by-side cylinders, an increase in P^* at a given Re may result in such a flow structure change (e.g., Refs. 22 and 44). An increased P^* means an enlarged gap and hence a gap flow of increased streamwise momentum, which is difficult to become biased. On the other hand, at a given P^*, the boundary layer on the gap side of each cylinder becomes thinner considerably with increasing Re,[25] again leading to an effectively enlarged gap and a gap flow of increased streamwise momentum. This explains why a smaller P^* needs a higher Re [e.g., 9×10^3 at $P^*=2.0$ and 2.5×10^3 at $P^*=2.5$, Fig. 13(f)] to change the biased flow or two distinct St to the nonbiased flow or single St. Note that both St differ little in their variation rate with respect to Re, owing to the fact that both cylinders are immersed in a uniform and undisturbed approaching flow. On the other hand, for type 3, the downstream cylinder is subjected to a nonuniform and disturbed approaching flow; therefore, the St value associated with the upstream cylinder is more sensitive to Re than that with the downstream cylinder.

At low Re, the E_u value of type 4C [Fig. 14(e)] appears quite similar to that of type 4B [Fig. 14(d)], exhibiting a pronounced peak at St=0.15 in the narrow street but at St =0.30 in the wide street, in conformity to the qualitatively same flow structures shown in Figs. 15(f) and 15(g). At a higher Re the pronounced peak in both E_u occurs at St =0.20 [Fig. 14(f)], corresponding to two coupled streets either antiphased or in-phased [Figs. 15(h) and 15(i)].

As P^* increases beyond 2.7, type 4C reaches the extreme, that is, the two distinct St at low Re collapse to St_0, at least for the Re range presently examined. E_u displays one dominant peak [Fig. 14(g)] at St=0.20. The variation in St exhibits the same trend as in an isolated cylinder wake, whose St reduces from $Re=3\times10^3$ to 2×10^4.[25,38–40] The flow of type 4D consists of two coupled vortex streets, either in antiphase or in phase [Figs. 15(j) and 15(k)].

V. DEPENDENCE OF St, THE St-Re RELATIONSHIP, AND FLOW STRUCTURE ON P^* AND α

Kiya *et al.*[4] and Hu and Zhou[6] showed the isocontours of St in the P^*-α plane at a fixed Re, which provided information on the dependence of St and the flow structure on P^* and α but not on the Re effect on this dependence. Figures 16 and 17 present the isocontours of St at two different Re, i.e., 1.5×10^3 and 2.0×10^4. Various types of the St-Re relationships are divided by dashed lines in the figures, and individual flow regimes, as classified by Hu and Zhou,[6] are separated by solid lines. The surface plots corresponding to the isocontours are also presented. It should be highlighted that the resolution of these contours is limited by the grid size of measurement points [Fig. 1(b)]. A number of observations can be made.

(1) It is evident that the two surface plots [Figs. 16(c) and 16(d)] of St associated with the downstream cylinder appear quite similar; in contrast, the two [Figs. 17(c) and 17(d)] associated with the upstream cylinder display a remarkable qualitative change, in particular, for the regions of types 3 and 4B or flow regimes S-II and T-I.[6] The observation suggests that the Reynolds number has a much more pronounced effect on the upstream-cylinder-generated wake than on the downstream-cylinder-generated wake, as noted in Sec. IV.

(2) In the P^*-α plane, type 1 occurs at small P^*, not exceeding 1.1–1.25, the exact value depending on α. On the other hand, type 2 corresponds to small α, not exceeding 10°. While the former corresponds well to the single-body flow mode, i.e., S-Ia as classified by Hu and Zhou,[6] the latter largely exhibits characteristics similar to the wake of two tandem cylinders[13] and occurs in the flow regime of S-Ib. Type 3 is located at intermediate P^* $[=(1.1-1.2)-(1.5-2.2)]$ and α $(=10°-75°)$ and occurs mostly in the flow regime of S-II. The P^* value of its upper border with type 4 decreases from 2.2 to 1.2 as α increases from 10° to 75° because a larger α corresponds to a smaller P^* for a given transverse width

Downloaded 17 Mar 2011 to 158.132.161.180. Redistribution subject to AIP license or copyright; see http://pof.aip.org/about/rights_and_permissions

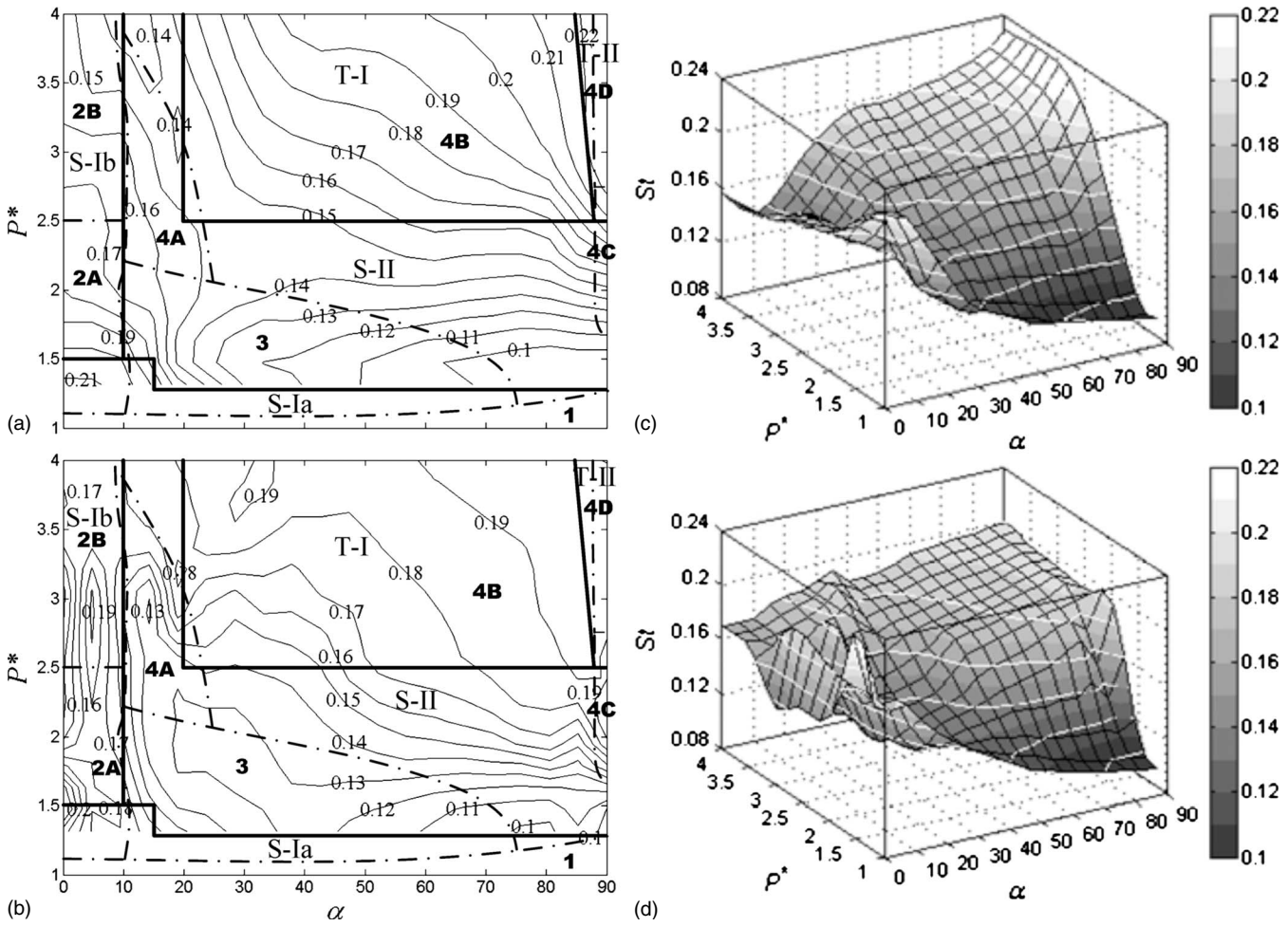

FIG. 16. The isocontours of St (thin solid lines) associated with the downstream cylinder: (a) $Re=1.5\times10^3$ and (b) 2.0×10^4. Dashed lines divide different types of the St-Re relationship and thick solid lines separate flow regimes classified by Hu and Zhou (Ref. 6) at $Re=7.0\times10^3$. The surface plots corresponding to (a) and (b) are presented in (c) and (d), respectively.

(which is linked to the gap flow strength or interactions between the shear layers) between the cylinders. Type 4 occupies the region of large P^* (>1.2–2.2) and corresponds to the flow modes of T-I, T-II, and the part of S-II of larger P^*. Type 4A takes the region of small α, i.e., 10°–20°; type 4B is in the region of larger α, i.e., 20°–88°; types 4C and 4D correspond to largest α (88°–90°), where the former occurs at intermediate P^* (1.7–2.7) and the latter at large P^* (>2.7).

(3) The highest St occurs for type 3 at $Re=1.5\times10^3$ and is associated with the upstream-cylinder-generated wake, when the downstream cylinder pushes the gap flow toward the upstream cylinder, generating a very narrow wake behind the upstream cylinder, with highly intensified interactions among the four shear layers [Fig. 12(a)]. On the other hand, the smallest St falls in the region of type 1 when the two cylinders are so close that they behave like a single body (Fig. 6).

(4) The isocontours in Fig. 16 are considerably more sparely separated than in Fig. 17, that is, the St associated with the upstream cylinder exhibits a stronger dependence on P^* and α than that with the downstream cylinder. Furthermore, the contours in Fig. 17 are densely distributed at $\alpha\lesssim20°$ or $P^*\lesssim2.0$, in particular, at the higher Re, indicating the regions where St is sensitive to P^* or α. On the other hand, the contours in Fig. 16 are sparsely distributed, except the region of $\alpha\lesssim12°$ at the higher Re, suggesting a relatively weak dependence of St, associated with the downstream cylinder, on P^* and α.

(5) The St range may vary rather wildly from one type of the St-Re relationship to another. Type 1 has a St of about 0.09 or 0.5 St_0, which is almost independent of Re (Fig. 4). The St ranges of types 2A and 2B are 0.17–0.24 and 0.14–0.23, respectively; the St associated with one cylinder is virtually the same as with the other. The difference in St between the upstream- and downstream-cylinder-generated wakes is maximum in type 3; at $Re=1.5\times10^3$, St is 0.36–0.68 for the upstream cylinder and 0.10–0.19 for the downstream cylinder. The large difference lies in the highly intensified interactions among the four shear layers at relatively smaller P^* and intermediate α [Figs. 12(a) and 12(c)]. With a relatively large P^*, type 4 occupies the region above type 3. As such, the interaction among the four shear layers is less intensified, resulting in a reduced difference in St between the downstream- and upstream-cylinder-generated

Downloaded 17 Mar 2011 to 158.132.161.180. Redistribution subject to AIP license or copyright; see http://pof.aip.org/about/rights_and_permissions

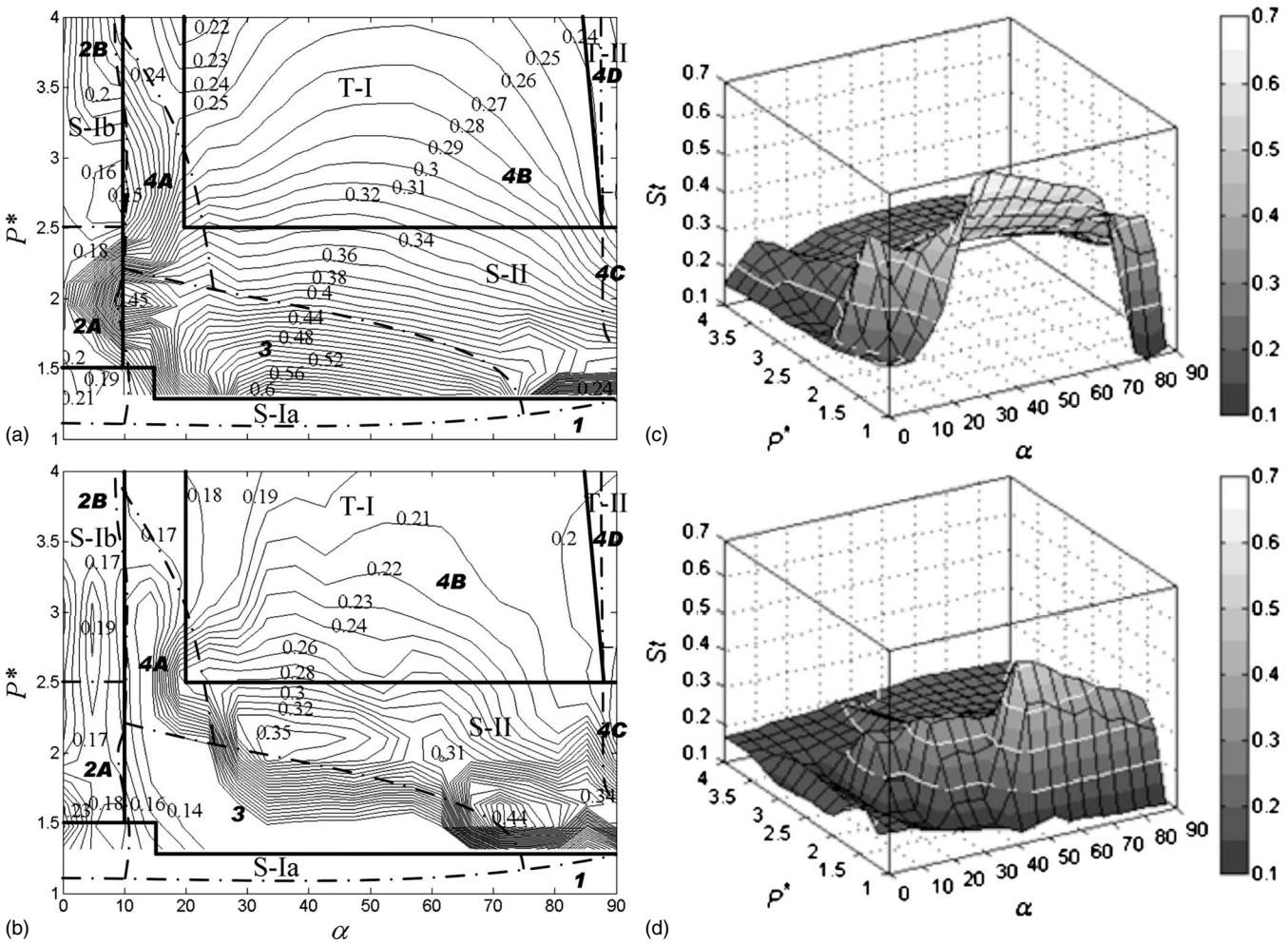

FIG. 17. The isocontours of St associated with the upstream cylinder: (a) $\mathrm{Re}=1.5\times10^3$ and (b) 2.0×10^4. The surface plots corresponding to (a) and (b) are presented in (c) and (d), respectively. The line types are as in Fig. 16.

wakes, compared with type 3; at $\mathrm{Re}=1.5\times10^3$, St is about 0.24–0.40 for the upstream cylinder and 0.10–0.22 for the downstream cylinder.

VI. CONCLUSIONS

The wake of two staggered cylinders is measured using two hotwires, with the incidence angle α ranging from 0° to 90°, the pitch-to-diameter ratio P^* from 1.2 to 4.0 and the Reynolds number Re from 1.5×10^3 to 2.0×10^4. The investigation focuses on the Re effect on St, the initial conditions (i.e., interactions between the four shear layers), and the flow structure. The measurements, along with those in literature, lead to following conclusions.

Four distinct types of the St-Re relationship are observed over the P^*-α plane examined. Type 1 is a single St that varies slightly with Re. Type 2 is again a single St, which displays a discontinuous rise as Re reaches a critical Reynolds number Re_c, between 6.5×10^3 and 9.5×10^3, depending on P^*. Type 3 is characterized by two distinct values of St. The higher St exhibits a strong dependence on Re, but the lower value does not. With increasing Re, the higher St collapses suddenly to the lower. Type 4 displays two distinct St at low Re; both change suddenly or progressively into St_0.

Type 1 occurs at $P^*<1.1-1.2$, depending on α. At such a small P^*, the gap flow between the cylinders plays a negligibly small role in flow development and the shear layers separate alternately from the outer side of the two cylinders, forming a single staggered vortex street of St=0.09.

Type 2 corresponds to the region of $\alpha<10°$ and $P^*>1.1-1.2$ and, in view of a difference in flow physics behind the discontinuous rise in St, may be divided into types 2A and 2B, corresponding to $P^*=1.1-2.5$ and 2.5–4, respectively. For type 2A, the shear layers separating from the upstream cylinder shoot over and roll up behind the downstream cylinder at $\mathrm{Re}<\mathrm{Re}_c$ but reattach on the downstream cylinder at $\mathrm{Re}>\mathrm{Re}_c$. For type 2B, the shear layers reattach on the downstream cylinder at $\mathrm{Re}<\mathrm{Re}_c$ but form vortices before reaching the downstream cylinder for $\mathrm{Re}>\mathrm{Re}_c$.

Type 3 occurs at $P^*=(1.1-1.2)-(1.5-2.2)$ and $\alpha=10°-75°$. At low Re, the inner shear layer separates from the upstream cylinder and runs through the gap between the cylinders; the gap flow is biased toward the upstream cylinder, resulting in a narrow street of higher St behind the upstream cylinder and a wide street of lower St behind the

Downloaded 17 Mar 2011 to 158.132.161.180. Redistribution subject to AIP license or copyright; see http://pof.aip.org/about/rights_and_permissions

downstream cylinder. As Re exceeds Re_c, with increased streamwise momentum, the inner shear layer reattaches on the downstream cylinder, resulting in the sudden disappearance of the narrow street and hence the higher St.

Type 4 occurs at larger P^* than type 3 and is divided into four subtypes. Type 4A corresponds to small α ($P^*=2.2-4.0$, $\alpha=10°-20°$). At low Re, the flow separating from the inner side of the upstream cylinder approaches and dives beneath the downstream cylinder. While the flow through the gap and the outer shear layer of the downstream cylinder form vortices at a lower St, the outer shear layer over the upstream cylinder forms vortices at a higher St. At $Re>Re_c$, the inner shear layer around the upstream cylinder rolls up, forming vortices between the cylinders. As such, the two wakes display similarity to that behind an isolated cylinder, with the two St collapsing rather suddenly into an intermediate value, close to St_0. Type 4B corresponds to a larger α ($20°<\alpha<88°$). Thus, the shear layer separated from the inner side of the upstream cylinder fails to reattach on the downstream cylinder. Naturally, the lower St rises slowly; meanwhile, the higher drops progressively, both approaching St_0. Type 4C falls in the regions of $P^*=1.7-2.5$ and $\alpha=88°-90°$. The gap flow is biased toward one cylinder. At adequately high Re, the gap flow is less biased, generating two antiphase or in-phase vortex streets. Type 4D occurs at larger P^* (>2.5) than type 4C, where the interference between the cylinders is small and the flow is characterized by two in-phase or antiphase vortex streets of the same St ($\approx St_0$).

Finally, the dependence of the Re-St relationship on P^* and α is provided, as compared to the classification of the flow structure.[6,9] This dependence, along with the isocontours and their characteristics of St in the P^*-α plane given at two representative Re, 1.5×10^3 and 2.0×10^4, may be used for the prediction of St in various engineering situations.

ACKNOWLEDGMENTS

Y.Z. wishes to acknowledge support given to him from the Research Grant Council of HKSAR through Grant No. PolyU 5334/06E and from The Hong Kong Polytechnic University through Grant No. G-YF30.

[1] M. M. Zdravkovich, "The effects of interference between circular cylinders in cross flow," J. Fluids Struct. **1**, 239 (1987).
[2] D. Sumner, S. J. Price, and M. P. Païdoussis, "Flow-pattern identification for two staggered circular cylinders in cross-flow," J. Fluid Mech. **411**, 263 (2000).
[3] Z. F. Gu and T. F. Sun, "On interference between two circular cylinders in staggered arrangement at high subcritical Reynolds numbers," J. Wind Eng. Ind. Aerodyn. **80**, 287 (1999).
[4] M. Kiya, M. Arie, H. Tamura, and H. Mori, "Vortex shedding from two circular cylinders in staggered arrangement," ASME J. Fluids Eng. **102**, 166 (1980).
[5] M. M. Zdravkovich, "Review of flow interference between two circular cylinders in various arrangements," ASME J. Fluids Eng. **99**, 618 (1977).
[6] J. C. Hu and Y. Zhou, "Flow structure behind two staggered circular cylinders. Part I: downstream evolution and classification," J. Fluid Mech. **607**, 51 (2008).
[7] D. Sumner and M. D. Richards, "Some vortex-shedding characteristics of the staggered configuration of circular cylinders," J. Fluids Struct. **17**, 345 (2003).
[8] M. M. Alam and H. Sakamoto, "Investigation of Strouhal frequencies of two staggered bluff bodies and detection of multistable flow by wavelets," J. Fluids Struct. **20**, 425 (2005).
[9] J. C. Hu and Y. Zhou, "Flow structure behind two staggered circular cylinders. Part II: Heat and momentum transport," J. Fluid Mech. **607**, 81 (2008).
[10] T. Igarashi, "Characteristics of the flow around two circular cylinders arranged in tandem (1st report)," Bull. JSME **24**, 323 (1981).
[11] T. Igarashi, "Characteristics of the flow around two circular cylinders arranged in tandem (2nd report)," Bull. JSME **27**, 2380 (1984).
[12] L. Ljungkrona and B. Sundén, "Flow visualization and surface pressure measurement on two tubes in an inline arrangement," Exp. Therm. Fluid Sci. **6**, 15 (1993).
[13] G. Xu and Y. Zhou, "Strouhal numbers in the wake of two inline cylinders," Exp. Fluids **37**, 248 (2004).
[14] H. J. Kim and P. A. Durbin, "Investigation of the flow between a pair of circular cylinders in the flopping regime," J. Fluid Mech. **196**, 431 (1988).
[15] S. J. Xu, Y. Zhou, and R. M. C. So, "Reynolds number effects on the flow structures behind two side-by-side cylinders," Phys. Fluids **15**, 1214 (2003).
[16] J. F. Huang, Y. Zhou, and T. M. Zhou, "Three-dimensional wake structure measurement using a modified PIV technique," Exp. Fluids **40**, 884 (2006).
[17] G. S. West and C. J. Apelt, "The effect of tunnel blockage and aspect ratio on mean flow past a circular cylinder with Reynolds number between 10^4 and 10^5," J. Fluid Mech. **114**, 361 (1982).
[18] L. Ljungkrona, C. H. Norberg, and B. Sundén, "Free-stream turbulence and tube spacing effects on surface pressure fluctuations for two tubes in an in-line arrangement," J. Fluids Struct. **5**, 701 (1991).
[19] D. Sumner, S. S. Wong, S. J. Price, and M. P. Païdoussis, "Fluid behavior of side-by-side circular cylinders in steady cross-flow," J. Fluids Struct. **13**, 309 (1999).
[20] D. Sumner, M. D. Richards, and O. O. Akosile, "Two staggered circular cylinders of equal diameter in cross-flow," J. Fluids Struct. **20**, 255 (2005).
[21] K. Kamemoto, "Formation and interaction of two parallel vortex streets," Bull. JSME **19**, 283 (1976).
[22] P. Bearman and A. J. Wadcock, "The interaction between a pair of circular cylinders normal to stream," J. Fluid Mech. **61**, 499 (1973).
[23] Z. J. Wang and Y. Zhou, "Vortex interactions in a two side-by-side cylinder near-wake," Int. J. Heat Fluid Flow **26**, 362 (2005).
[24] A. Roshko, "Experiments on the flow past a circular cylinder at very high Reynolds numbers," J. Fluid Mech. **10**, 345 (1961).
[25] M. M. Zdravkovich, *Flow Around Circular Cylinders: Fundamentals* (Oxford Science, New York, 1997), Vol. 1.
[26] M. M. Alam, H. Sakamoto, and Y. Zhou, "Determination of flow configurations and fluid forces acting on two staggered circular cylinders of equal diameter in cross-flow," J. Fluids Struct. **21**, 363 (2005).
[27] M. M. Alam and Y. Zhou, "Strouhal numbers, forces and flow structures around two tandem cylinders of different diameters," J. Fluids Struct. **24**, 505 (2008).
[28] S. M. Bloor, "The transition to turbulence in the wake of a circular cylinder," J. Fluid Mech. **19**, 290 (1964).
[29] O. M. Griffin, "The unsteady wake of an oscillating cylinder at low Reynolds number," ASME J. Appl. Mech. **38**, 523 (1971).
[30] Y. Zhou and M. W. Yiu, "Flow structure, momentum and heat transport in a two-tandem-cylinder wake," J. Fluid Mech. **548**, 17 (2006).
[31] A. Okajima, "Strouhal number of rectangular cylinders," J. Fluid Mech. **123**, 379 (1982).
[32] H. Nakaguchi, K. Hasimoto, and S. Muto, "An experimental study of aerodynamic drag on rectangular cylinders," J. Jpn. Soc. Aeronaut. Space Sci. **16**, 1 (1968).
[33] Y. Otsuki, K. Washizu, H. Tomizawa, and A. Ohya, "A note on the aeroelastic instability of a prismatic bar with square section," J. Sound Vib. **34**, 233 (1974).
[34] M. M. Alam, M. Moriya, K. Takai, and H. Sakamoto, "Fluctuating fluid forces acting on two circular cylinders in a tandem arrangement at a subcritical Reynolds number," J. Wind Eng. Ind. Aerodyn. **91**, 139 (2003).
[35] S. Ishigai, E. Nishikawa, E. Nishimura, and K. Cho, "Experimental study of structure of gas flow in tube banks axes normal to flow," Bull. Jpn. Soc. Mech. Eng. **15**, 949 (1972).
[36] A. Prasad and C. H. K. Williamson, "The instability of the shear layer separating from a bluff body," J. Fluid Mech. **333**, 375 (1997).

Downloaded 17 Mar 2011 to 158.132.161.180. Redistribution subject to AIP license or copyright; see http://pof.aip.org/about/rights_and_permissions

[37] Y. Couder and C. B. Basdevant, "Experimental and numerical study of vortex couples in two-dimensional flows," J. Fluid Mech. **173**, 225 (1986).
[38] A. Roshko, "On the development of turbulent wakes from vortex streets," NACA Report No. TN 2913, 1953 (downloaded from http://authors.library.caltech.edu/428/).
[39] C. Norberg, "Flow around a circular cylinder: Aspect of fluctuating lift," J. Fluids Struct. **15**, 459 (2001).
[40] C. H. K. Williamson, "Vortex dynamics in the cylinder wake," Annu. Rev. Fluid Mech. **28**, 477 (1996).
[41] S. M. Bloor and J. H. Gerrard, "Measurements on turbulent vortices in a cylinder wake," Proc. R. Soc. London, Ser. A **299**, 319 (1966).
[42] J. H. Gerrard, "Experimental investigation of separated boundary layer undergoing transition to turbulence," Phys. Fluids **10**, S98 (1967).
[43] M. F. Unal and D. R. Rockwell, "On vortex formation from a cylinder. Part 1. The initial instability," J. Fluid Mech. **190**, 491 (1988).
[44] M. M. Alam, M. Moriya, and H. Sakamoto, "Aerodynamic characteristics of two side-by-side circular cylinders and application of wavelet analysis on the switching phenomenon," J. Fluids Struct. **18**, 325 (2003).

Downloaded 17 Mar 2011 to 158.132.161.180. Redistribution subject to AIP license or copyright; see http://pof.aip.org/about/rights_and_permissions